Mechanical properties and thermal stability of reactive arc evaporated Ti-Cr-Al-N coatings

Rikard Forsén

Linköpings universitet

Abstract

This licentiate thesis reports experimental and theoretical work on the high temperature mechanical properties and the thermal stability of cubic (c)-$(Ti-Cr-Al)_1$-N_1 coatings. It is demonstrated that it is possible to tailor and improve the properties of hard nitride coatings by different degrees of multicomponent alloying. When Cr is added to Ti-Al-N the coatings exhibit age hardening up to 1000 ℃ which is higher compared to what is observed for Ti-Al-N. In addition, the coatings show a less pronounced hardness decrease when hexagonal (h)-Al-N is formed compared to Ti-Al-N. The improved thermal stability is discussed in terms of a lowered coherency stress and a lowered enthalpy of mixing due to the addition of Cr. When Ti is added to Cr-Al-N the formation and growth of the detrimental h-Al-N phase is suppressed and delayed improving the mechanical properties. This is discussed in terms of kinetic effects where the Ti atoms obstruct the Al diffusion and consequently the growth of h-Al-N precipitates. The microstructure evolution investigated at different stages of spinodal decomposition, coarsening and phase transformations are correlated to the thermal responses and the mechanical hardness of the coatings. Upon annealing up to 1400 ℃ the coatings decompose into c-TiN, bcc-Cr and h-AlN. The decomposition takes place via several intermediate phases, c-CrAlN, c-TiCrN and hexagonal (β)-Cr_2N.

   The oxidation resistance of $(Ti_x-Cr_y-Al_{60})_1$-N_1 is also investigated and presented for different x/y ratios. The results show that it is possible to generate coatings with both excellent mechanical properties and oxidation resistance improving the functionality in the working temperature range of 850-1100 ℃ of for example cutting tools.

Preface

This is a summary of the work I have performed in the Nanostructured Materials group at the Department of Physics, Chemistry and Biology (IFM) at Linköping University between January 2010 and July 2012. The main focus of this wok has been to study the high temperature mechanical properties and the thermal stability of reactive arc evaporated Ti-Cr-Al-N coatings. The depositions have been carried out at Seco Tools AB in Fagersta and the ERDA characterization has been carried at Uppsala University. The work has been supported by Seco Tools AB and the SSF project Designed multicomponent coatings, Multifilms.

My contributions to the included papers

Paper I

Improving thermal stability of hard coating films via a concept of multicomponent alloying

H. Lind, **R. Forsén**, B. Alling, N. Ghafoor, F. Tasnádi, M. P. Johansson, I. A. Abrikosov, and M. Odén

Appl. Phys. Lett. 99, 091903 (2011)

I took part in the execution of the depositions and the experimental characterizations and took part in the planning and the compilation of the paper.

Paper II

Decomposition and phase transformation in TiCrAlN thin coatings

R. Forsén, M. P. Johansson, M. Odén and N. Ghafoor

Submitted for publication

I took part in the planning of the depositions, carried out the depositions and the experimental characterizations and I wrote the paper.

Paper III

Improved mechanical properties in oxidation resistant AlCrN coatings through Ti addition

R. Forsén, M. P. Johansson, M. Odén and N. Ghafoor

In manuscript

I planned the work, performed the depositions and the experimental characterization and I wrote the paper.

Acknowledgements

بسم الله الرحمن الرحيم

Magnus Odén, my supervisor

Naureen Ghafoor and Mats Johansson, my co-supervisors

Hans Lind, Ferenc Tasnádi, Björn Alling and Igor Abrikosov for valuable contributions to my papers

Colleagues in the Nanostructured Materials, Thinfilm physics, Plasma and Coatings physics and Theoretical physics groups

Everyone who has helped me at Seco Tools in Fagersta

Family and friends, especially my parents and my wife

Table of content

1. Introduction

1.1 Coatings

By using coatings it is possible to combine the properties of a bulk material and the properties of the coating. Coatings are used for a wide range of applications in today's society, for example to improve electrical contact, corrosion resistance, mechanical properties or as decorative thin films.[1] As an art it has been used for decorative purposes for several thousands of years.[2] By means of modern deposition techniques it is possible to deposit a coating in a metastable state or even an unstable state which may give more favorable properties compared to the stable state found in nature. It might also exhibit favorable properties during its decomposition into its stable state. When the temperature is increased the atoms have higher kinetic energy and thus have a higher chance to rearrange into a more stable phase. The most stable phase will always prevail but the temperature will control at which rate the decomposition occurs. In the cutting tool industry protective coatings have been used since late 1960s [3,4] and around 90 % of the cemented carbide inserts used today are coated [5]. Coated cutting tools can have up to 10 times increased lifetime compared to tools without any protective coating. One of the early material systems used for protective coatings of cutting tools was Ti-N. Due to continuously higher demands on cutting speed, feeding rates and to minimize the usage of cooling lubricants this material system has to a large extent been replaced by Ti-Al-N. Ti-Al-N has been used in industry since the 1980s [6,7] and is well known in the literature [8-14]. It shows superior mechanical properties at elevated temperatures compared to Ti-N [6,7,12,13]. Thanks to a very beneficial phase transformations of

unstable Ti-Al-N coatings occurring at working temperatures of the cutting tool the mechanical properties are improved. This improvement upon high temperature exposure is called age hardening and for this particular material system it is observed in applications during which the temperature reaches 800-1000 ºC [15,16]. When the temperature is too high during cutting the Ti-Al-N coating undergoes unfavorable phase transformations and the mechanical properties deteriorate. It is therefore desirable to find a way to improve the thermal stability of Ti-Al-N coatings to be able to push the cutting performance even further. Attempts to increase the thermal stability of Ti-Al-N have recently been made by adding a third metal, Y, Nb, Hf or B, to the materiel system [17,18] while another approach was through a concept of multilayer growth [9], where the coating architecture affects the decomposition process. For Ti-Cr-Al-N it has been shown that the addition of Cr gives a higher hardness and lower wear rates.[19-21] However the fundamental mechanisms that yield these good properties are not yet understood.

At higher temperatures oxidation can also become a problem and lead to a deceased cutting performance. Cr-Al-N is a material system that shows superior oxidation resistance compared to Ti-Al-N.[22] However Cr-Al-N coatings do not demonstrate the aforementioned age hardening to the same extent as in Ti-Al-N.[23] This means that Cr-Al-N coatings have a lower hardness at working temperatures during metal cutting and are therefore not suited for high abrasive applications.

This work sets out to investigate and to enhance the understanding of the thermal stability and the mechanical properties of Ti-Cr-Al-N. To make the understanding of this quaternary material system less difficult the first approach has been to use the well

4

known Ti-Al-N and Cr-Al-N material systems as references. With small additions of Cr and Ti to these material systems the fundamental mechanisms have been experimentally investigated and coupled to theoretical work conducted in parallel. The experimental investigations in this work have been obtained with techniques such as transmission electron microscopy (TEM), x-ray diffraction (XRD), differential scanning calorimetry (DSC), thermogravimetric analysis (TGA) and nanoindentation. With these techniques the extracted experimental findings include information from a micrometer scale down to an atomic scale. Based on first principle calculations the mixing enthalpy and the local tendencies for spinodal decomposition in c-TiCrAlN have also been calculated.

1.2 Aim and layout

The aim of this work is to provide a fundamental understanding of the high temperature mechanical properties, thermal stability and microstructure of reactive arc evaporated Ti-Cr-Al-N coatings with different compositions. This thesis includes chapters with general theory and information about the materials and characterization techniques that are relevant for this work. The results from this work are presented in the papers included in this thesis.

2. Stability and phase transformations

All systems are continuously striving for minimization of their energy. If long enough time is given to any system it will eventually transform into its most stable form in a given environment. Materials found in nature are normally very stable. After millions of years since their formation the material has had long time to minimize its energy in its surrounding environment. However some materials might have been formed under high temperatures or high pressures for example solid crystalline rocks found inside mountains or oil deep down in the ground. The external parameters and the long time are both needed to create these phases. But even if the oil is pumped up and exposed to atmospheric pressure and lower temperatures or the crystalline rock is refined and separated the material may remain in their original state for an extremely long time. The relative energies of different phases will only determine the magnitude of the forces that may drive a transformation. This means that it is not possible to assume the material will always be in its most stable form. Something must prevent the system from transforming into a lower energy state immediately. Mathematically this can be described as a local minimum in the energy.

The energy of a system may have several different local minima corresponding to many different phases. In figure 1 the Gibbs free energy of a system is depicted. The system has a local minimum in point E surrounded by energy barriers which the system has to overcome before the system can transform into state D with lower energy. The barriers can for example arise from the spatial rearrangement of the atoms or the creation of a compositional gradient requiring some amount of energy.

Generally speaking, if the system is not in its global minimum there is a driving force for lowering the energy and at higher temperatures the transformation is faster due to the higher kinetic energy of the atoms.
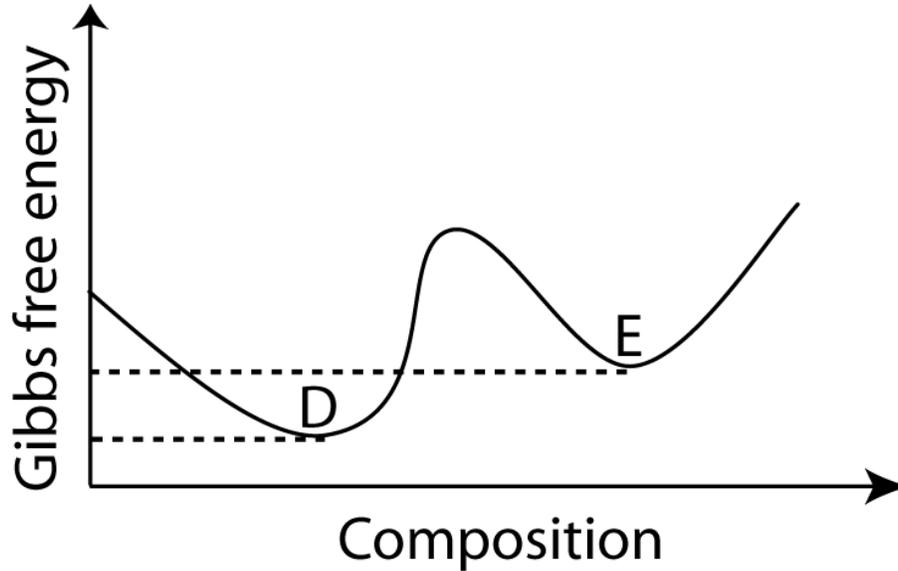

Figure 1 showing the Gibbs free energy of an arbitrary system with two local minima D and E.

In this work different compositions of c-Ti-Cr-Al-N have been studied. This system is unstable but remains in its unstable state for a very long time unless the temperature is increased. The reason for this can be found by studying its mixing enthalpy where miscibility gaps can be identified and remembering that there is also an energy barrier for diffusion.

2.1 Mixing enthalpy and miscibility gaps in c-Ti-Cr-Al-N

If two or more immiscible components are mixed together the energy increases. But because of the aforementioned diffusion barriers it is possible to synthesis a material in such a state. In figure 2 the mixing enthalpy of *c*-Ti-Cr-Al-N [24] at zero Kelvin and 1000 ºC is shown. The mixing free energy was calculated using first principles calculations and the configurational entropy within the mean-field approximation[10].

Mixing enthalpy: $\Delta G = G(Ti_x Cr_y Al_z N) - xG(TiN) - yG(CrN) - zG(AlN)$
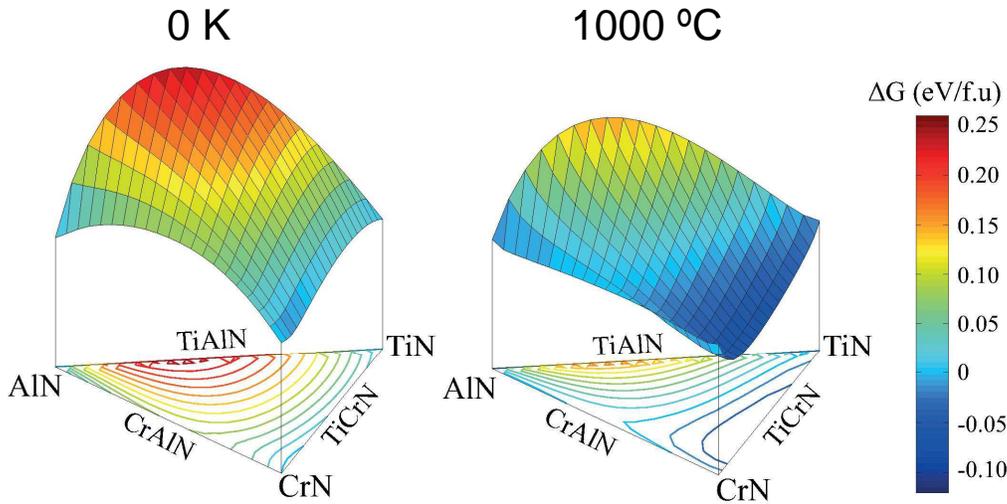

Figure 2 containing the mixing enthalpy of *c*-Ti-Cr-Al-N at zero Kelvin and 1000 ºC.

At zero Kelvin it can be seen that the mixing enthalpy has positive values for almost all compositions. The most immiscible component is *c*-Al-N with the largest gap versus *c*-Ti-N. By increasing to Cr-content the system becomes less unstable. Ternary *c*-Ti-Cr-N is more or less stable for all compositions. The most stable components in the system are the binary phases, *c*-Ti-N, *c*-Cr-N and *c*-Al-N. However, these calculations are only

performed for a cubic crystal structure and *c*-Al-N is not stable. Therefore there is a driving force for transformation of *c*-Al-N into its stable form, *h*-Al-N. At 1000 ℃ the mixing enthalpy is overall lower compared to zero Kelvin and is in fact negative along the Ti-Cr-N ternary. It is therefore not expected that *c*-Ti-Cr-N would decompose at high temperatures. But *c*-Cr-N has however two more stable phases, hexagonal *β*-Cr$_2$-N and *bcc*-Cr to which it transforms at higher temperatures.

The decomposition of this quaternary material system or any other alloy occurs with one important condition. The initial overall composition remains constant since no new elements are created nor destroyed. If the initial composition is Ti$_x$Cr$_y$Al$_z$N then x+y+z is a constant. This means that if for example the Al content decreases somewhere in the coating it has to increase somewhere else. This will only happen if it leads to an overall decrease of the energy. There is one condition under which any change in composition will lead to an overall energy decrease. Such a region is called a spinodal and it can be identified in the mixing enthalpy of *c*-Ti-Cr-Al-N.

2.2 Spinodal decomposition

At points B and C in figure 3 the second derivative of the Gibbs free energy is zero corresponding to where the slope is at maximum. This means that between points B and C, for any change in the composition, the sum of the energy difference in all those domains where the energy increases will always be lower than the sum of the energy difference where the energy decreases. Thus, between points B and C any compositional fluctuation will always lead to an overall energy decrease. This region is called the spinodal and can be mathematically defined for one component as $\dfrac{\partial^2 G}{\partial^2 x} < 0$.
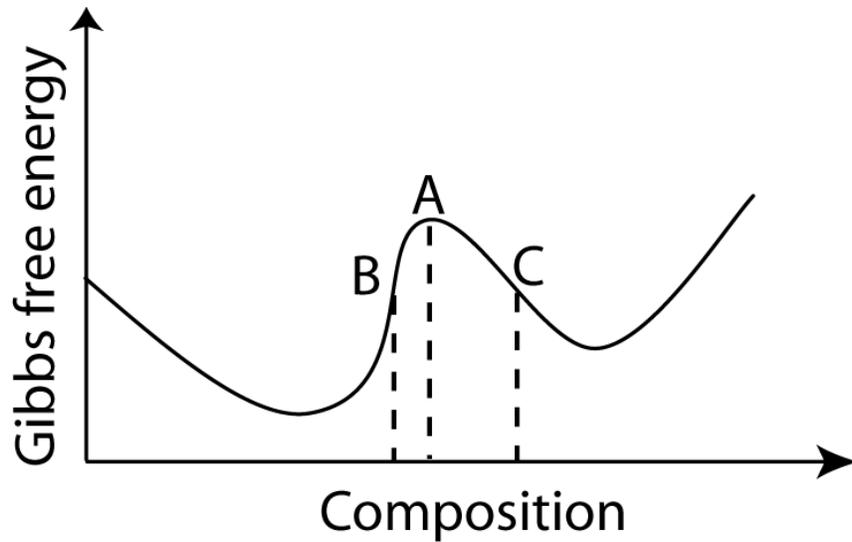
Figure 3 showing the Gibbs free energy versus composition of an arbitrary system with a local maximum in point A and a spinodal region between points B and C.

If the composition of a system is defined by point A in figure 3 its energy is a local maximum and lies within the spinodal region. Here the system is unstable without any barriers since any compositional change will lower the energy and therefore no nuclei are needed to initiate the segregation of the elements. This is in contrast to the case when the composition lies between the spinodal region and a local minimum. In such region nuclei are needed to commence the segregation and growth. This kind of decomposition is therefore called nucleation and growth. An elemental segregation that takes place within the spinodal region is called spinodal decomposition and leads to a microstructure with some typical characteristics. The segregation occurs uniformly in the material with a constant size of the different domains that are formed. The degree of the compositional change within the domains is however changing with time. As it turns out the compositional change versus distance can be described by a sinusoidal function, see figure 4. Due to the sinusoidal appearance the domain size is often referred to as wavelength and the composition as amplitude.
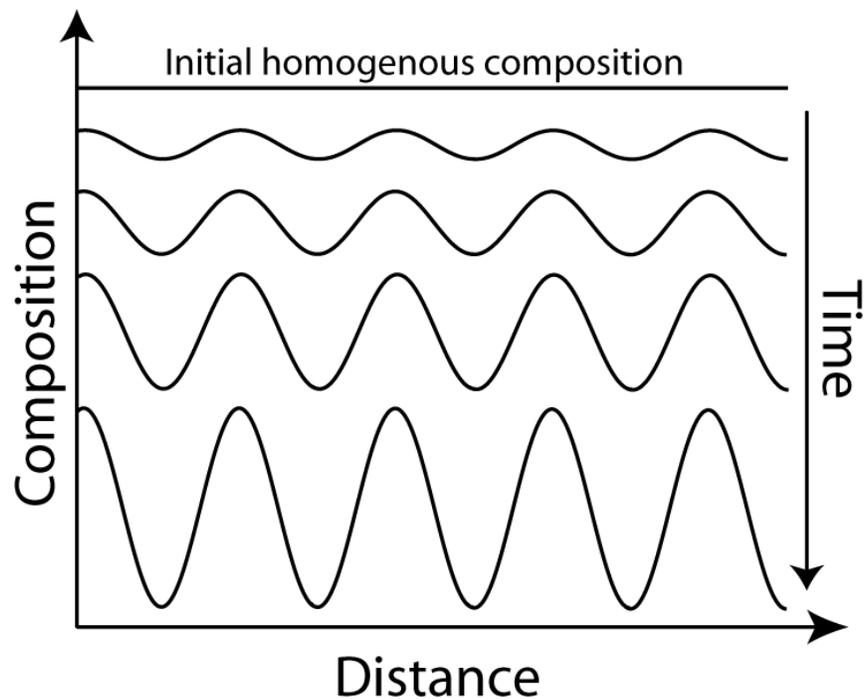
Figure 4 showing the compositional modulation versus distance at different times during spinodal decomposition.

It should be noted that a coarsening process during which the energy is decreased further usually follows the spinodal decomposition. The presented microstructure results in this work are mainly from the coarsening stage after post deposition annealing. This is because the small wavelength (less than a few nanometers) during the spinodal decomposition makes it difficult to observe with the analytical instruments that have been used. Additionally, at high temperatures around 1000-1100 ℃ relevant for cutting tool operations the spinodal decomposition occurs very fast and the onset of the coarsening process begins almost instantaneously. Spinodal decomposition can result in a hardness increase upon exposure to high temperatures. This is referred to as age hardening.

2.3 Age hardening

When coatings are deposited using reactive cathodic arc evaporation the densities of vacancies and dislocations are often very high. This yields high hardness of the coatings in their as deposited state due to the coating's non equilibrium state. When the temperature is increased the number of vacancies and dislocations is lowered and the hardness decreases. This process is referred to as recovery. The recovery is an irreversible process and can therefore be observed with *ex-situ* measurements after post deposition annealing.
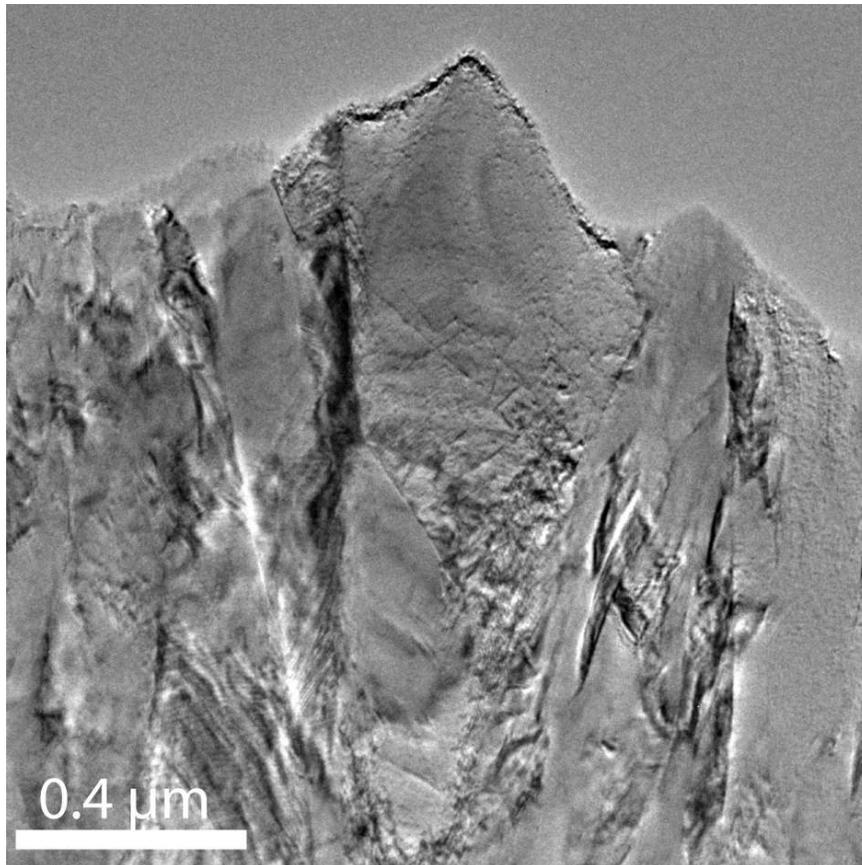

Figure 5 shows an overview TEM micrograph of a catohdic arc evaporated Ti-Cr-Al-N coating in its as deposited state. The growth is columnar with a high density of defects and dislocations.

The hardness of different coatings is of interest in this work because it is a factor influencing the performance of the coating and the cutting tool during metal machining. Most interesting is the high temperature hardness since the metal machining operation generates very high temperatures. The hardness is strongly related to dislocation movement, i.e. plastic deformation. The hardness can be improved by introducing different means to obstruct the movement of the dislocations. For example, the dislocation movements can be altered if nanometer sized coherent regions with different composition and elastic constants are formed in the material. Spinodal decomposition is one mechanism to form such regions.

Because of the different lattice parameters of c-Cr-N, c-Ti-N and c-Al-N there is an increasing strain energy associated with the coherent segregation of the elements during the spinodal decomposition of c-Ti-Cr-Al-N. The strain increases the force required for a dislocation to pass the domains with different compositions. Thus, the movement of the dislocations is obstructed and the material becomes harder. The requirement for this mechanism is that the domains remain coherent otherwise the strain is reduced and the hardening effect is lost. When the domain size is increasing during the coarsening the strain becomes too large and above some critical size misfit dislocations are introduced reducing the strain. The material is then over aged and results in a lower hardness.[12,14] Figure 6 shows the hardness versus annealing temperature of different Ti-Cr-Al-N alloys. Cr-Al-N [23] only exhibits a recovery process while Ti-Al-N [9] and Ti-Cr-Al-N show different degrees of age hardening and over ageing are observed.
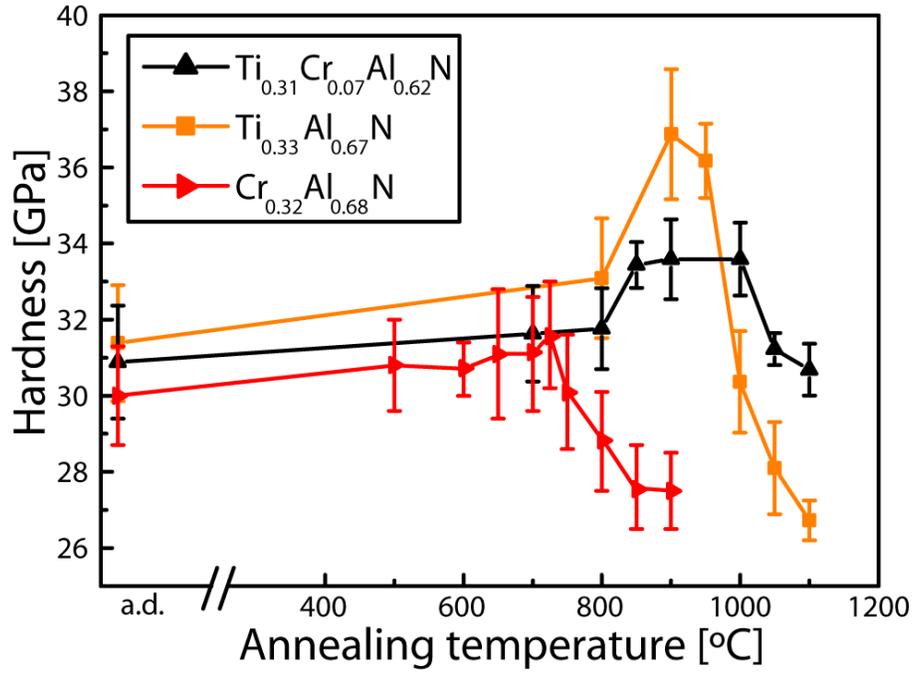
Figure 6 shows the hardness versus annealing temperature of Cr-Al-N[23], Ti-Al-N[9] and Ti-Cr-Al-N. Cr-Al-N shows only the healing process whereas Ti-Al-N and Ti-Cr-Al-N show different degrees of age hardening and over ageing.

3. Synthesis

There are many different techniques to deposit thin films and coatings. Some techniques are better suited for certain applications than others. Some of the properties that will determine which technique is best suited include for example, film thickness, adhesion, shape and dimensions of the substrate, electrical conductivity of the deposited material and the substrate, level of acceptable impurities in the film etc. In general the same material deposited with different techniques will have different properties. But also the other way around, the properties achieved with the same technique will depend on things such as different properties of the deposited material system, substrate material, impurities etc. Furthermore, by changing one parameter, for example substrate bias, it may affect many other parameters such as the plasma density, temperature, composition in the film, stress levels etc. These changes can have dramatic consequences for the properties and performance of the film. The general relationships between the parts that are dealt with within the field of thin film physics are described in equation 1. This equation is often referred to as the material science paradigm.

Synthesis $\longleftrightarrow$ Structure and Composition $\longleftrightarrow$ Properties eq. 1

From equation 1 it can be seen that if certain thin film properties are wished for the structure and composition of the film have to be in accordance and in order to get the structure and composition right the deposition process has to be conducted accordingly. The equivalence goes for all three sides of the equation. For example, to achieve a

particular structure requires the correct deposition process which will also determine the properties of film.

  Cathodic arc evaporation belongs a category of physical vapor deposition (PVD) techniques where sputtering is also a common technique.[25]. It is desired to have a high level of ionization to get a dense coating and to be able to control the impact energy and thus the surface mobility of the impinging atoms by changing the substrate bias.[26] Using cathodic arc evaporation the degree of ionization is very high.[27] For sputtering the ionized fraction of the deposited material is very low, however the technique can be improved by sputtering in a so called high power impulse mode (HIPIMS) [28] but the cost is a lower deposition rate [29]. All the coatings deposited in this work have been performed using an industrial cathodic arc evaporation system.

3.1 Cathodic arc evaporation

The metal material used in the coating is fabricated into a solid piece called cathode and may consist of either one pure element or a mixture of different elements. In order to transport the material from the cathode to the substrate at a reasonable rate and to avoid impurities in the coating the deposition takes place in vacuum. In reactive mode where for example nitrogen is introduced in order to deposit a nitride the nitrogen pressure is in the range of a few Pa. To start the process a very high current is fed through the cathode surface using a metal trigger rod. The high current density results in a local dielectric breakdown of the material and causes a small part to melt and evaporate.[30] In order to have a continuous flow of ejected species the location of the arc spot at the cathode surface is controlled and moved by a magnet behind the cathode. The arc spot is kept

rotating and oscillate over the surface to eject material from different parts. In this process anything from single atoms to big micrometer sized chunks of material are ejected. The larger pieces of material are referred to as macro particles. These macroparticles will be deposited in the coating and will affect the properties of the coating. The macroparticles can be avoided in the coating using filters between the cathode and the substrate but this come at a high cost of lowering the deposition rate.[31] The continuously high current density in the cathode provides high enough energy to ionize the ejected species from the cathode. The result is a mix of freely moving charged particles, called plasma [32], between the cathode and the substrate. The successfulness of the process is also dependent on the material that is evaporated. Pure Al cathodes are for example very difficult to use for cathodic arc evaporation because of its low melting temperature.

4. Materials

In this work different compositions of the coatings have been deposited using the same deposition technique under fixed parameters. To achieve the different compositions in the coatings different combinations of compound cathodes have been used. Strictly speaking, different compositions of the cathodes will also influence the deposition parameters such as ion charge distributions and surface mobility. It is also known that different elements will evaporate more easily with different rates in different directions.[33] These effects are neglected in this work and the focus is on the yielded compositions as measured with energy dispersion x-ray spectroscopy (EDX) and elastic recoil detection analysis (ERDA). All studied coatings in this work are quaternary nitrides containing different parts of Ti-N, Cr-N and Al-N with a nitrogen content of 50 ± 1 %. The ternary systems Ti-Al-N and Cr-Al-N are well studied and commonly used for cutting tool applications. These two ternary material systems have acted as references during this work. Here follows a summary of the properties of these material systems which are relevant for this work.

4.1 Ti-Al-N

Ti-Al-N has excellent mechanical properties at elevated temperatures and is widely used as a protective coating of cutting tools.[6,7]. The mechanical properties and the oxidation resistance increases with higher Al content as long as a cubic structure can be maintained. But if the Al content is too high h-Al-N is formed and as a consequence the mechanical properties deteriorate. Therefore compositions close to $Ti_{0.33}Al_{0.67}N$ is typically used to avoid h-Al-N while optimizing the properties. Al was added to the previously used Ti-N system with the intention to improve its poor oxidation resistance.[34,35] The great

improvement of the mechanical properties when adding Al was initially attributed to the protective aluminum oxide layer formed at the surface of the coating.[6,7] The oxide layer at the surface acts as a barrier for the oxygen atoms to diffusion further into the coating and thus improving its mechanical properties.[36] This mechanism surely affects the mechanical properties in a positive way but nowadays it is not considered to be the major mechanism behind the improved properties and the observed age hardening in this material system. Instead the explanation can be found in the mixing enthalpy of c-Ti-Al-N which is positive and contains a spinodal region meaning this is an unstable system. It is therefore expected to transform into a more stable form upon exposure to high temperatures which is the mechanisms behind the age hardening.[10,12-14] With around 70 % of Al content the mixing enthalpy is close to its maximum within the spinodal region. Thus any infinitesimal change in composition will lead to an overall decreased energy and therefore no nucleation site is required to initiate the segregation of Ti-N and Al-N. Upon exposure to high temperatures either during metal cutting or during annealing, the Ti and Al atoms begin to segregate while maintaining one single crystal structure. The result of the spinodal decomposition is coherent nanometer sized c-Al-N- and c-Ti-N-enriched domains. This segregation is associated by stress due to the different elastic properties and the different lattice parameters of c-Al-N and c-Ti-N[11]. Because of this generated stress propagation of dislocations is obstructed and results in an increased hardness as explained in chapter 2.3.

If the coating is continuously exposed to high temperatures a coarsening process starts to take place after the spinodal decomposition. During the coarsening the energy is reduced by lowering the surface to volume ratio of the c-Al-N and c-Ti-N domains.

When the domain interface becomes small in comparison to the domain size the coherency stress is relaxed by formation of dislocations. This is accompanied by a transformation of the *c*-Al-N into the more stable *h*-Al-N phase. These events lead to a dramatic decrease in hardness.[37] Still Ti-Al-N coatings provide good abrasive wear protection of cutting tools. The decomposition route of Ti-Al-N can be expressed according the equation 2.

|	
c-Ti-Al-N → *c*-Ti-N+*c*-Al-N → *c*-Ti-N + *h*-Al-N *~800 ºC* *~1000 ºC*	**eq. 2**
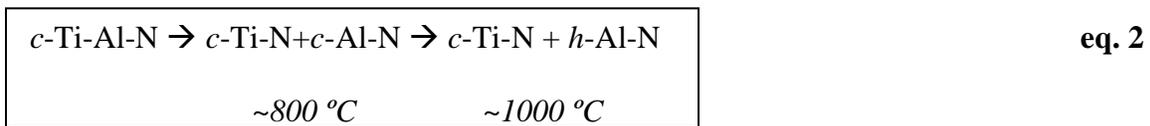
For applications where the oxidation resistance is more important than the high temperature mechanical properties Cr-Al-N is a better choice compared to Ti-Al-N.

4.2 Cr-Al-N

Cr-N coatings are widely used in plastic molding operations and metal forming to protect the tool from corrosion and oxidation.[38] Just like what is done to improve the mechanical properties of Ti-N coatings, Al can be added to Cr-N coatings forming a ternary system.[39] With Al addition protective layers of chromium and aluminum oxide are formed at the coating surface preventing diffusion of oxygen deeper into the coating and in terms of corrosion and oxidation resistance Cr-Al-N coatings are superior to Ti-Al-N.[22] *c*-Cr-Al-N coatings can be deposited with up to 60-70 at. % of Al. If the Al concentration is higher *h*-Al-N will form and the hardness decreases.[40,41] It has been reported that the cubic phase can be retained up to two hours of annealing at 900 ℃.[40] Also, results from $Cr_{0.32}Al_{0.68}N$ [23] coatings show a weak age hardening process [12,13]

due to Al-N precipitation at ~700 ℃ but at higher temperatures the mechanical properties deteriorate. The reason why the high temperature mechanical properties are worse for Cr-Al-N than for Ti-Al-N is that the mixing enthalpy and its curvature of c-Cr-Al-N is less compared to c-Ti-Al-N.[11,24] Thus when c-Cr-Al-N is exposed to high temperatures a coherent decomposition like for Ti-Al-N does not take place.[23,42] The positive enthalpy in the system will only lead to formation and growth of h-Al-N precipitates in the vicinity of grain boundaries where the diffusion is high enough. When these h-Al-N precipitates grow the hardness is decreased rapidly at relatively low temperatures compared to Ti-Al-N.[23,42] Since the temperature at the edge of a cutting tool during metal machining can reach beyond 1000 ℃ [43], Cr-Al-N protective coatings are inadequate for high temperature and high abrasive applications. The decomposition route of Cr-Al-N can be expressed according to equation 3.

c-Cr-Al-N $\rightarrow$ c-Cr-Al-N+h-Al-N   **eq. 3**

$\sim$*700 ℃*
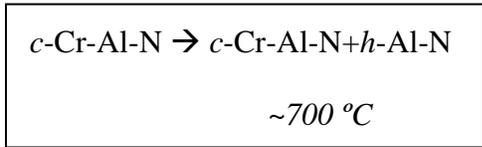
4.3 Ti-Cr-Al-N

Ti-Cr-Al-N is a commercially available material system today used as protective coating of cutting tools. Various studies have shown that the performance of these coatings can outperform Ti-Al-N, for example during dry sliding tests.[19-21,44]. The fundamental mechanisms that yield these good properties were not understood at the beginning of this work. The high temperature mechanical properties, thermal response, microstructure and phase evolution of this quaternary system have been characterized and are presented in the papers included in this thesis.

5. Characterization

5.1 Transmission Electron microscopy

It is known from the Rayleigh criterion that the smallest distance that can be resolved is proportional to the wavelength of the radiation. Therefore the resolution of light optical microscopes is limited by the wavelength of visible light, $\sim 10^{-7}$ m. When electrons are accelerated to 200 kV the wavelength of the electron radiation is around $\sim 10^{-12}$ m. This is a theoretical improvement of five orders of magnitude compared to a light optical microscope. The true resolution is however limited by lens imperfections of the microscope. The development of new microscopes and correction techniques is continuously going on and with the most advanced transmission electron microscopes today Angstrom resolution can be achieved.

Since the mean free path of electrons in solid material is very short, $\sim 10^{-9}$, the sample has to be very thin. Sample preparation is not just tedious routine work, good sample preparation is essential to benefit from the high theoretical resolution that the microscope may have. If features with a size of a few nanometers are about to be studied the sample thickness should be on the same scale. If the sample is too thick the projected image generated while the electrons are transmitted through the material will contain information from overlapping features. Once a thin sample has been prepared it is possible to observe and measure things such as compositional fluctuations down to an atomistic scale, lattice parameters and diffraction patterns obtained from nanometer-sized areas.

5.2 X-Ray diffraction

In contrast to the time consuming sample preparation required before using transmission electron microscopy X-ray diffraction measurements require almost no preparation. And by using photon radiation instead of electrons the measurement does not have to be carried out in vacuum. By focusing light in the X-ray wavelength region of $\sim 10^{-10}$ m onto the sample the incidence radiation will be backscattered spherically in all directions by the atoms in the sample. If there is some kind of periodicity among the atoms in the sample the scattered radiation will interfere constructively in some directions. The constructive interference can be measured by focusing the scattered light on an x-ray detector. Constructive interference will occur when the path length difference between scattered light from different inter atomic planes correspond to a multiple of the wavelength of the x-ray source. When applying this technique the lattice parameter or the interatomic distances in the sample can be extracted since the wavelength and the geometry are known variables. By measuring the distance between the atoms in a sample the crystal structure and the phases present in the sample can be determined.

5.3 Thermal analysis

All the coatings in this work are deposited in a metastable state. The mechanical properties of coatings are directly coupled to what microstructure they have. When metastable coatings are exposed to high temperatures the atoms begin to diffuse and rearrange to more stable positions with less energy. This will lead to phase transformations and microstructural changes in the coatings. The result of a phase transformation or any other reaction in the coating is that heat energy is either released,

an exothermic reaction, or absorbed, an endothermic reaction. These two reaction types can be measured *in-situ* with a technique called differential scanning calorimetry **(DSC)**. The sample is heated with a predefined heating rate. When there is an exothermic or an endothermic reaction occurring in the sample the energy required to raise the temperature of the sample is either increased or decreased. Together with the sample also a reference sample with a known thermal response is heated. The output signal from the instrument is the difference in energy required to raise the temperature between the samples. This allows subtracting known reactions that might occur in both samples and only look at the differences between the samples.

In this work the reference material is simply an empty inert sapphire sample holder that remains stable without any reactions up to the studied temperatures of 1400 ºC. To compensate for the energy requirement between heating the holders of the measured sample and the empty holder a second heating cycle is always performed. During the first heating it is assumed that the occurring reactions, e.g. the phase transformations, are irreversible meaning that after the first heating cycle the coating is in a more stable state or possibly its equilibrium state and no more reactions will occur. The second heating cycle is then used for background subtraction to clearly see where the reactions in the coating occur.

Since the coating is very thin in comparison to the substrate the signal from the substrate would completely dominate the signal if they were measured together. Therefore the substrate has to be removed in order to measure the thermal response of the coating. This is a very tedious work. In fact, the work required to prepare one DSC sample exceeds the work required for transmission electron microscopy and has to be

planned already at the deposition stage. The preparation begins by depositing the coating onto Fe foils with a preferably very thick thickness around ~10 µm. The Fe foils are electrically conductive and this is a requirement to be able to apply and maintain a constant bias potential to the substrate. The Fe foils are also mechanically strong enough to withstand the mechanical stress induced by the coating during the deposition. The coated Fe foils are thereafter mechanically grinded and dissolved in hydrochloric acid. Luckily, the studied coatings in this work were unaffected by the hydrochloric acid but it might not be the case for other material systems. The result is a powder sample ready for thermal analysis.

5.4 Nanoindentation

Hardness is defined as the resistance against plastic deformation [45] and nanoindentation is a method used to determine the hardness of thin films. A diamond tip is indented into the film while continuously observing the load. The tip has a known contact area versus its penetration depth. If the tip leaves a plastic deformation not deeper than 10 % of the coating thickness the deformation can be assumed to be independent of the substrate and the hardness of the coating can be determined as the force divided by the cross section area of the tip.

  When measuring the hardness of coatings that have been deposited using cathodic arc evaporation special care has to be taken to avoid areas containing the aforementioned macro particles. These residues from the deposition process impose defects in the lattice and will affect the mechanical properties in their vicinity. The coating surface is usually

also relatively rough in comparison to the coating result of other deposition techniques such as sputtering. Therefore the surface has to be polished prior to measurement. To avoid complete removal of the coatings when the samples are polished they are mounted with a tampered angle in a sample holder to only partially remove the coating. The indentation sites are then carefully chosen using an optical microscope to avoid the micrometer sized particles.

6 Summary of the included papers

Paper I

The mixing enthalpy and the driving force for spinodal decomposition in c-Ti-Cr-Al-N is calculated based on first principle calculations. The mixing enthalpy strongly depends on the ratio between its metal components. The mixing enthalpy is most sensitive to the Al component. Ti-Al-N has the highest mixing enthalpy within a spinodal for almost all compositions except close to the binaries. Cr-Al-N also has a positive mixing enthalpy but with much lower curvature and with absence of a spinodal region. For Ti-Cr-N the mixing enthalpy is more or less zero. This work has investigated and predicted the decomposition routes that low Cr content Ti-Cr-Al-N coatings take. The most striking result is that c-Ti-Cr-Al-N decomposes via the metastable phase c-Cr-Al-N. It is also shown that because of this intermediate step in the decomposition route the mechanical properties are enhanced.

Paper II

In this paper a detailed experimental verification of the results in the first paper is presented. It is shown that since the lattice parameter of Cr-N lies in between Ti-N and Al-N the driving force for relaxation of the coherent domain boundaries is reduced during decomposition. This results in a less pronounced age hardening but also in a less pronounced hardness decrease since the domains remain coherent at higher temperatures. The decomposition route is determined as follows: c-Ti-Cr-Al-N $\rightarrow$ c-Ti-Cr-N + c-Cr-Al-N $\rightarrow$ c-Ti-Cr-N + h-Al-N $\rightarrow$ c-Ti-N + β-Cr$_2$N+ h-Al-N$\rightarrow$ c-Ti-N + bcc-Cr + h-Al-N. It is

verified that the driving force for spinodal decomposition is lowered with increasing Cr content. This results in an extended time duration of the spinodal decomposition which delays the onset of the coarsening. Because of the delayed coarsening the domain boundaries are maintained coherent at even higher temperatures resulting in higher hardness at temperatures of 1000-1100 ºC. Additionally, it is also shown that by increasing the Cr content (<17 at. %) formation of h-AlN in grain boundaries is promoted.

Paper III

In paper III the influence of Ti addition to Cr-Al-N in terms of mechanical properties and oxidation resistance is investigated. The results show that the high temperature mechanical properties can be drastically improved through Ti addition. The decomposition takes place via a nucleation and growth process. The Ti addition suppresses and delays the formation and growth of h-Al-N resulting in improved hardness. The oxidation resistance is negatively affected by the Ti addition due the promotion of TiO_2 over the more prtective α-Al_2O_3. However, it is possible to generate coatings that outperform ternary Ti-Al-N in terms of both oxidation resistance and mechanical properties at elevated temperatures.

References

[1] L. Martinu and D. Poitras, J. Vac. Sci. Technol. A 18 (6) (2000) 2619.

[2] E.D. Nicholson, Gold Bulletin 12 (4) (1979) 161.

[3] T. Childs, Metal machining: theory and applications, Arnold, 2000.

[4] Modern skärande bearbetning: en praktisk handbok, Sandvik Coromant, 1995.

[5] P.H. Mayrhofer, C. Mitterer, L. Hultman, H. Clemens, Progr. Mater. Sci. 51 (8) (2006) 1032.

[6] O. Knotek, M. Bohmer, T. Leyendecker, J. Vac. Sci. Technol. A 4 (6 , Nov.-Dec. 1986) (1986) 2695.

[7] H.A. Jehn, S. Hofmann, V. Ruckborn, W. Munz, J. Vac. Sci. Technol. A 4 (6) (1986) 2701.

[8] A. Knutsson, M.P. Johansson, P.O.Å. Persson, L. Hultman, M. Odén, Appl. Phys. Lett. 93 (14) (2008)

[9] A. Knutsson, M.P. Johansson, L. Karlsson, M. Od́n, J. Appl. Phys. 108 (4) (2010)

[10] B. Alling, A.V. Ruban, A. Karimi, O.E. Peil, S.I. Simak, L. Hultman, I.A. Abrikosov, Phys. Rev. B 75 (4) (2007)

[11] B. Alling, T. Marten, I.A. Abrikosov, A. Karimi, J. Appl. Phys. 102 (4) (2007)

[12] A. Hörling, L. Hultman, M. Odén, J. Sjölén, L. Karlsson, J. Vac. Sci. Technol. A 20 (5) (2002) 1815.

[13] A. Höling, L. Hultman, M. Odén, J. Sjölén, L. Karlsson, Surf. Coat. Technol. 191 (2-3) (2005) 384.

[14] P.H. Mayrhofer, A. Hörling, L. Karlsson, J. Sjölén, T. Larsson, C. Mitterer, L. Hultman, Appl. Phys. Lett. 83 (10) (2003) 2049.

[15] R. M'Saoubi, C. Le Calvez, B. Changeux, J.L. Lebrun, Proc. Inst. Mech. Eng. Pt. B: J. Eng. Manuf. 216 (2) (2002) 153.

[16] M.A. Davies, T. Ueda, R. M'Saoubi, B. Mullany, A.L. Cooke, CIRP Ann. Manuf. Technol. 56 (2) (2007) 581.

[17] R. Rachbauer, D. Holec, M. Lattemann, L. Hultman, P.H. Mayrhofer, International J. Mater. Res. 102 (6) (2011) 735.

[18] K. Kutschej, N. Fateh, P.H. Mayrhofer, M. Kathrein, P. Polcik, C. Mitterer, Surf. Coat. Technol. 200 (1-4) (2005) 113.

[19] S.G. Harris, E.D. Doyle, A.C. Vlasveld, J. Audy, J.M. Long, D. Quick, Wear 254 (1-2) (2003) 185.

[20] Z.F. Zhou, P.L. Tam, P.W. Shum, K.Y. Li, Thin Solid Films 517 (17) (2009) 5243.

[21] A.I. Kovalev, D.L. Wainstein, A.Y. Rashkovskiy, G.S. Fox-Rabinovich, K. Yamamoto, S. Veldhuis, M. Aguirre, B.D. Beake, Vacuum 84 (1) (2009) 184.

[22] M. Kawate, A.K. Hashimoto, T. Suzuki, Surf. Coat. Technol. 165 (2) (2003) 163.

[23] H. Willmann, P.H. Mayrhofer, L. Hultman, C. Mitterer, J. Mater. Res. 23 (11) (2008) 2880.

[24] H. Lind, R. Forsén, B. Alling, N. Ghafoor, F. Tasnádi, M.P. Johansson, I.A. Abrikosov, M. Odén, Appl. Phys. Lett. 99 (9) (2011) 091903.

[25] Handbook of deposition technologies for films and coatings: science, technology and applications, Noyes, 1994.

[26] S.M. Rossnagel, Journal of Vacuum Science and Technology B: Microelectronics and Nanometer Structures 16 (5) (1998) 2585.

[27] J. Vyskocil and J. Musil, J. Vac. Sci. Technol. A 10 (1992) 1740.

[28] V. Kouznetsov, K. Macák, J.M. Schneider, U. Helmersson, I. Petrov, Surf. Coat. Technol. 122 (2–3) (1999) 290.

[29] U. Helmersson, M. Lattemann, J. Bohlmark, A.P. Ehiasarian, J.T. Gudmundsson, Thin Solid Films 513 (1-2) (2006) 1.

[30] D.M. Mattox, Met Finish 100 (1 SUPPL.) (2002) 394.

[31] I.G. Brown, Annual Revi. Mater. Sci. 28 (1) (1998) 243.

[32] M.A. Lieberman and A.J. Lichtenberg, Principles of Plasma Discharges and Mater. Process., John Wiley & Sons, 2005.

[33] A.O. Eriksson, J.Q. Zhu, N. Ghafoor, M.P. Johansson, J. Sjölen, J. Jensen, M. Odén, L. Hultman, J. Rosén, Surf. Coat. Technol. 205 (15) (2011) 3923.

[34] B. Navinšek, P. Panjan, A. Cvelbar, Surf. Coat. Technol. 74-75 (PART 1) (1995) 155.

[35] J.C. Knight, Wear 138 (1–2) (1990) 239.

[36] B. Kim, Y. Kim, J. Nah, J. Lee, J. Vac. Sci. Technol. A 17 (1) (1999) 133.

[37] M. Odén, L. Rogström, A. Knutsson, M.R. Terner, P. Hedström, J. Almer, J. Ilavsky, Appl. Phys. Lett. 94 (5) (2009)

[38] J. Vetter, Surf. Coat. Technol. 76-77 (PART 2) (1995) 719.

[39] O. Knotek, M. Atzor, A. Barimani, F. Jungblut, Surf. Coat. Technol. 42 (1) (1990) 21.

[40] A.E. Reiter, V.H. Derflinger, B. Hanselmann, T. Bachmann, B. Sartory, Surf. Coat. Technol. 200 (7) (2005) 2114.

[41] H. Hasegawa and T. Suzuki, Surf. Coat. Technol. 188-189 (1-3 SPEC.ISS.) (2004) 234.

[42] H. Willmann, P.H. Mayrhofer, P.O.Å. Persson, A.E. Reiter, L. Hultman, C. Mitterer, Scr. Mater. 54 (11) (2006) 1847.

[43] H.O. Gekonde and S.V. Subramanian, Surf. Coat. Technol. 149 (2-3) (2002) 151.

[44] Q. Luo, W.M. Rainforth, L.A. Donohue, I. Wadsworth, W. Münz, Vacuum 53 (1-2) (1999) 123.

[45] ASM handbook. Vol. 8, Mechanical testing and evaluation, ASM International, 2000.